Empirical Estimation of Intra-Cellular Volume Fraction in Mouse Spinal Cord with Q-Space Diffusion MRI

H. H. Ong[1], and F. W. Wehrli[1]

[1]Laboratory for Structural NMR Imaging, Department of Radiology, University of Pennsylvania School of Medicine, Philadelphia, PA, United States

Introduction

Changes in neural white matter (WM) intra- and extra-cellular volume fraction (ICF and ECF) are important for characterization of WM injury and pathology. For example, in multiple sclerosis ICF is decreased due to axon loss. Diffusion MRI techniques are valuable for non-destructively assessing WM micro-architecture as diffusing water molecules are sensitive to local structure. Current diffusion MRI techniques measure WM ICF by multi-exponential curve fitting or numeric Laplace inversion of the signal decay[1] or fitting the decay to a model[2]. However, the former approach is a difficult ill-posed inverse problem, while the latter requires *a priori* assumptions in the model. An experiment that empirically measures WM ICF would circumvent both dilemmas. Malmborg et al[3] recently proposed such an experiment in which multiple signal decay curves are obtained at the same q-values ($q = (2\pi)^{-1}\gamma G\delta$, where G and δ are the diffusion gradient amplitude and pulse length, respectively) while varying diffusion gradient pulse duration. Diffusion in the ICF and ECF are expected to be restricted and Gaussian, respectively[2], and have different dependences on δ[4]. Gaussian diffusion is unaffected by changes in δ, while restricted diffusion exhibits less signal decay with increasing δ. ICF can be directly inferred from a comparison of the decay curves. In this work, we use the procedure outlined by Malmborg et al to measure the ICF of WM tracts in healthy mouse spinal cords (SC), which have a simple WM structure to facilitate interpretation, and compare the results with histology.

Method

Five SC cervical sections (C6-C7) were dissected from perfusion-fixated 8-10 month-old female C57 BL/6 mice. Experiments were performed with a custom-built 50 T/m z-gradient coil in conjunction with a solenoidal RF coil set (4-turn, 3*mm* i.d.) interfaced to a 9.4 T spectrometer/micro-imaging system (Bruker DMX 400 with Micro2.5 gradients and BAFPA40 amplifiers). A diffusion-weighted stimulated-echo sequence was used: 64×64, sw=25kHz, TR=2s, TE/Δ=17.4/10*ms*, FOV/THK=4/1*mm*, and an ambient temperature of 19 °C. Two experiments were run with δ = 0.4 and 5*ms* yielding echo attenuations $E(\delta=0.4ms)$ and $E(\delta=5ms)$, respectively. The diffusion gradient was applied along the z-axis (perpendicular to SC long axis) in 64 increments of q (q_{max}=0.82 μm^{-1}). q-Space decay curves were obtained for each pixel and averaged over ROIs (20 pixels, after zero-filling image to 256×256) selected within the seven WM tracts (Figure 1). As described in [3], the signal attenuation value at which $E(\delta=0.4ms)$ and $E(\delta=5ms)$ begin to deviate from each other, P_d, provides a relaxation-weighted estimate of ICF. Unlike in [3], P_d was taken to be the value of $E(\delta=5ms)$ *immediately prior* to where the ratio $E(\delta=5ms)/E(\delta=0.4ms)$ >1.2, because when the ratio >1.2, the decay curves have already deviated (see Figure 2). After experiments, 0.5μm SC sections from the MRI image slice were stained for myelin (toluidine blue) and optical microscopic images were obtained from all WM tracts. The images were then segmented into extra- and intra-axonal, and myelin regions with a custom watershed and profile based algorithm. ICF was taken to be the area of both the intra-axonal and myelin regions (see Discussion).

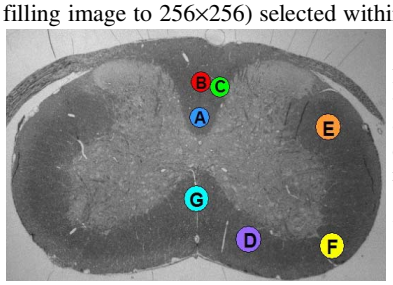

Figure 1. Optical image of SC section showing WM tract locations: A) dorsal corticospinal (dCST), B) gracilis (FG), C) cuneatus (FC), D) rubrospinal (RST), E) spinothalamic (STT), F) reticulospinal (ReST), G) vestibulospinal (VST).

Results and Discussion

ANOVA was run on histologic ICFs and no significant differences were detected among WM tracts. Therefore, for each specimen, in both experiments and histology, a single ICF was calculated by averaging all WM tract ICFs. Figure 3 shows a plot of histologic vs experimental ICFs. There is significant inter-specimen variation and the ICFs fall within the expected range of 60-80%. There is excellent linearity and correlation between histologic and experimental ICFs. The ICFs averaged over all specimens also show good agreement with each other.

The exact relaxation weighting effect on P_d is unclear. Perhaps due to the short TE used, ECF and ICF signals did not decay significantly (ECF and ICF T_2s are reported to be 78 and 300 ms, respectively[5]) and relaxation effects were minimized. Further, as the technique only differentiates between restricted and Gaussian diffusion, histologic ICF included both intra-axonal and myelin regions since the myelin water is restricted by the myelin sheaths. Finally, our histologic results offer a validation of the ICF measurement technique not available in [3]. Choosing to use SC allowed the diffusion gradient to be oriented orthogonal to the WM tracts for accurate ICF measurement. However, this technique can be readily applied to tortuous WM tracts in the brain with a tensor analysis[6].

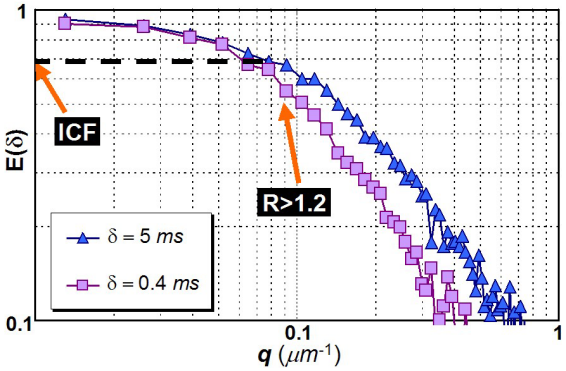

Figure 2. Sample VST $E(\delta=0.4ms)$ and $E(\delta=5ms)$ curves on logorithmic axes from a single specimen. **R** = $E(\delta=0.4ms)/E(\delta=5ms)$. Left arrow indicates the value used for ICF.

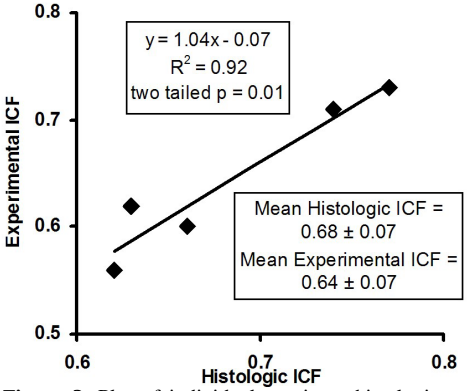

Figure 3. Plot of individual specimen histologic vs experimental ICFs with equation of line of best fit and mean values.

Conclusion

This work validates a previously proposed diffusion MRI technique to measure WM ICF and suggests that ICF may be measured to high accuracy non-destructively.

References: 1. Whittal K, et al, *JMR*, **84**:134–152 (1989). 2. Assaf Y, et al, *MRM*, **52**:965-978 (2002). 3. Malmborg C, et al, *JMR*, **180**:280-285 (2006). 4. Mitra PP, et al, *JMR A*, **113**:94-101 (1995). 5. Peled S, et al, *MRM*, **42**:911-918 (1999). 6. Assaf Y, et al, *MRM*, **47**:115-126. **Acknowledgements:** NIH grant R21 EB003951